Electronic Supplementary Information:

Distinctive Modulation of Halogen on Optical Anisotropy in α/β-Cd-P-X (X = Cl, Br, I)

Kewang Zhang,[a] Junben Huang,[b] Zhikang Chen,[a] Bei Zhang,[a] Ming-Hsien Lee,[c] Jun Zhang*[a]

[a] School of Physics Science and Technology, Xinjiang University, Urumqi, Xinjiang 830046, China.

[b] School of Materials Science and Engineering and Key Lab of Non-Ferrous Metal Materials Science and Engineering, Ministry of Education, Central South University, Changsha 410083, Hunan, China.

[c] Department of Physics, Tamkang University, New Taipei 25137, Taiwan

*Corresponding author E-mail: zhj@xju.edu.cn.

Contents

Nonlinear optical properties

The NLO coefficient is crucial for materials to be applied as second harmonic generation (SHG) conversion crystals. Theoretical NLO coefficients of the target compounds were also performed (listed in Table S1). For α-Cd_2P_3X (X= Cl, Br, I), the largest NLO coefficients are d_{33} = 1.39, d_{33} = 1.02, and d_{33} = 1.94 pm/V, respectively. Unfortunately, the relatively weak SHG response is probably associated with the structural arrangement. To analyze the contribution of an ion (or ionic group) to the SHG response, the SHG-density technique is adopted. It was performed by using the effective SHG of each band as a weighting coefficient to sum the probability densities of all states. The SHG-density caused by ion can be clearly viewed through occupied and unoccupied states, however, the states that do not contribute to SHG response will be invisible. SHG-density can be divided into occupied and unoccupied virtual-electron (VE) and virtual-hole (VH), respectively. The contributions of VE and VH of α-Cd_2P_3Cl, α-Cd_2P_3Br, and α-Cd_2P_3I were 40% and 60%, 57% and 43%, 43% and 57%, respectively (Figure S4). Provides a plot of the predominant contribution from X (X = Cl, Br, I) atoms along in occupied states. As for unoccupied states, SHG-density is concentrated on P atoms. What is more remarkable is that all compounds exhibit the increasing tendency of NLO coefficients which is consistent with their incremental hyperpolarizability because the going up halogen atoms size brings more contribution to the SHG effect (Table 1). Similar regularity can be observed in the cesium germanium halide perovskites $CsGeX_3$ (X = Cl, Br and I).[1]

Table S1 Calculated NLO coefficients of NCS α-Cd_2P_3X (X = Cl, Br, I) and the largest first-order hyperpolarizabilities $|\beta_{max}|$ of $[CdP_3X]$ groups.

Compounds	NLO coefficients (pm/V)	$\|\beta_{max}\|$ (a.u.)
α-Cd_2P_3Cl	d_{11} = −0.96, d_{15} = 0.12, d_{12} = −0.09, d_{13} = 0.78, d_{24} = 0.53, d_{33} = 1.23	2118.30
α-Cd_2P_3Br	d_{11} = −0.58, d_{15} = −0.39, d_{12} = −0.18, d_{13} = −0.82, d_{24} = −0.41, d_{33} = 1.33	3936.25
α-Cd_2P_3I	d_{11} = −0.08, d_{15} = −0.21, d_{12} = −0.42, d_{13} = -0.75, d_{24} = −0.07 d_{33} = 1.93	4557.03

Table S2 Crystallographic structure data of the title compounds.

Compounds	Space group	Band gap (eV)			Symmetry	Volume (Å^{-3})	Unit cell dimensions (Å)
		GGA	HSE06	Exp.			
α-Cd_2P_3Cl[2]	*Cc*	1.28	1.99	/	NCS	531.24	7.969(1), 8.984(2), 7.554(2)
α-Cd_2P_3Br[2]	*Cc*	1.24	1.93	1.90[2]	NCS	544.11	8.077(1), 9.088(2), 7.534(3)
α-Cd_2P_3I[2]	*Cc*	1.27	1.85	1.83[2]	NCS	569.84	8.243(1), 9.334(2), 7.516(2)
β-Cd_2P_3Cl[3]	*C*2/*c*	1.29	1.98	1.87[3b]	CS	532.62	7.988(1), 8.988(1), 7.555(1)
β-Cd_2P_3Br[3]	*C*2/*c*	1.26	1.91	1.86[3b]	CS	544.95	8.089(1), 9.089(1), 7.535(1)
β-Cd_2P_3I[3]	*C*2/*c*	1.26	1.89	1.74[3b]	CS	568.93	8.255(1), 9.304(1), 7.514(1)
Hg_2P_3Cl[4]	*C*2/*c*	1.12	1.86	/	CS	519.91	7.834(2), 8.844(11),7.591(1)
Hg_2P_3Br[4]	*Pbcn*	0.83	1.71	/	CS	558.16	8.014(1), 8.903(1), 7.823(1)

Table S3 Calculated birefringence Δn and optical permittivities $\Delta\varepsilon$ ($f \rightarrow$ infinity) of α/β-Cd_2P_3X (X = Cl, Br, I).

Compounds	**Space group**	ε_{xx}	ε_{yy}	ε_{zz}	$\Delta\varepsilon$	Δn
α-Cd_2P_3Cl	*Cc*	7.24	7.35	8.87	1.63	0.25
α-Cd_2P_3Br	*Cc*	7.81	7.84	9.08	1.27	0.19
α-Cd_2P_3I	*Cc*	9.18	9.13	9.48	0.35	0.04
β-Cd_2P_3Cl	*C*2/*c*	7.22	7.36	8.86	1.64	0.24
β-Cd_2P_3Br	*C*2/*c*	7.87	7.86	9.09	1.23	0.17
β-Cd_2P_3I	*C*2/*c*	9.25	9.17	9.54	0.37	0.03

Table S4 Birefringence and band gap of a series of excellent halide optical crystals.

Compounds	Space group	Band gap (eV)	Birefringence (@ 1064 nm)
$HgBr_2$[5]	*Cmc*2$_1$	3.30	0.24
HgI_2[6]	*Cmc*2$_1$	2.37	0.50
Hg_2Cl_2[7]	*I*4/*mmm*	2.90	0.54/0.55 (Exp.)
Hg_2Br_2[7]	*I*4/*mmm*	2.50	0.70/0.67 (Exp.)
Hg_2I_2[8]	*I*4/*mmm*	2.10	1.08/0.95 (Exp.)
$CsGeCl_3$[9]	*R*3*m*	3.67	0.000
$CsGeBr_3$[10]	*R*3*m*	2.32	0.001
$CsGeI_3$[11]	*R*3*m*	1.60	0.002
$CsPbCl_3$[12]	*Pnma*	2.66 (Cal.)	0.104
$CsPbBr_3$[12]	*Pnma*	2.17 (Cal.)	0.179
$CsPbI_3$[13]	*Pnma*	2.13	0.275
$(Cu(PS_3As_3)_4)Cl$[14]	*P*31*c*	2.89 (Cal.)	0.021
$(Cu(PS_3As_3)_4)Br$[14]	*P*31*c*	2.45 (Cal.)	0.024
$NaSb_3F_{10}$[15]	*P*6$_3$	4.97	0.100
$NaSb_3Cl_{10}$*[16]	*P*6$_3$	4.49 (Cal.)	0.170
$NaSb_3Br_{10}$*[16]	*P*6$_3$	3.72 (Cal.)	0.235
$NaSb_3I_{10}$*[16]	*P*6$_3$	2.59 (Cal.)	0.367
SbF_3[17]	*Cmm*2	4.29	0.145
$SbCl_3$*[16]	*Cmm*2	4.05 (Cal.)	0.212
$SbBr_3$*[16]	*Cmm*2	3.30 (Cal.)	0.295
SbI_3*[16]	*Cmm*2	1.95 (Cal.)	0.924
$Sn_2B_5O_9Cl$[18]	*Pnn*2	3.53	0.189/0.168 (Exp.) @ 546 nm
$Sn_2B_5O_9Br$[19]	*Pnn*2	3.11	0.464/0.439 (Exp.) @ 546 nm
$Sn_2B_5O_9I$*[19]	*Pnn*2	2.99 (Cal.)	0.70 @ 546 nm
$Pb_2B_5O_9Cl$[20]	*Pnn*2	3.96	0.081/0.067 (Exp.) @ 546 nm
$Pb_2B_5O_9Br$[21]	*Pnn*2	3.30	0.118/0.130 (Exp.) @ 546 nm
$Pb_2B_5O_9I$[22]	*Pnn*2	3.10	0.32 @ 546 nm
$Pb_6Ba_2(BO_3)_5Cl$[23]	*C*2/*m*	3.70	0.16 @ 532 nm
$Pb_6Ba_2(BO_3)_5Br$[23]	*C*2/*m*	3.60	0.18 @ 532 nm

* Represents hypothetical crystal.

Table S5 Static polarization and polarization anisotropy of $CsPbX_3$ (X = Cl, Br, I).

Compound	Space group	Species	Δα	Static polarization					
				xx	*xy*	*yy*	*xz*	*yz*	*zz*
$CsPbCl_3$	*Pnma*	$PbCl_6$	1.25	66.40	0.24	66.69	0.11	0.65	66.72
$CsPbBr_3$	*Pnma*	$PbBr_6$	2.36	95.29	1.07	95.98	−0.03	0.76	95.88
$CsPbI_3$	*Pnma*	PbI_6	8.46	146.09	−1.38	144.24	−3.68	−2.49	147.14

Table S6 Cut ionic radius for α/β-Cd_2P_3X (X = Cl, Br, I) and Hg_2P_3Cl.

Compound	Atom	Charge	Cut radius (Å)
α-Cd_2P_3Cl	Cd	+2	1.27
	P	−1	1.46
	Cl	−1	1.41
α-Cd_2P_3Br	Cd	+2	1.27
	P	−1	1.43
	Br	−1	1.50
α-Cd_2P_3I	Cd	+2	1.28
	P	−1	1.46
	I	−1	1.62
β-Cd_2P_3Cl	Cd	+2	1.27
	P	−1	1.43
	Cl	−1	1.43
β-Cd_2P_3Br	Cd	+2	1.27
	P	−1	1.45
	Br	−1	1.50
β-Cd_2P_3I	Cd	+2	1.28
	P	−1	1.47
	I	−1	1.73
Hg_2P_3Cl	Hg	+2	1.26
	P	−1	1.15
	Cl	−1	1.55

Table S7 Born effective charges of α/β-Cd_2P_3X (X = Cl, Br, I).

Compound	Atoms	q_{xx}	q_{yy}	q_{zz}	Δq
α-Cd_2P_3Cl	Cd_1	2.264	2.178	2.175	−0.002
	Cd_2	2.285	2.174	2.190	0.016
	Cl	−1.998	−1.879	−1.071	0.808
	P_1	−0.876	−0.811	−1.418	−0.607
	P_2	−0.786	−0.831	−0.440	0.391
	P_3	−0.890	−0.830	−1.437	−0.607
α-Cd_2P_3Br	Cd_1	2.41	2.33	2.19	−0.140
	Cd_2	2.39	2.33	2.17	−0.164
	Br	−2.11	−2.07	−1.06	1.011
	P_1	−0.91	−0.88	−1.44	−0.565
	P_2	−0.87	−0.86	−0.44	0.416
	P_3	−0.92	−0.87	−1.43	−0.558
α-Cd_2P_3I	Cd_1	2.69	2.65	2.19	−0.466
	Cd_2	2.67	2.65	2.17	−0.487
	I	−2.30	−2.34	−1.04	1.302
	P_1	−0.99	−0.99	−1.42	−0.434
	P_2	−1.08	−0.99	−0.48	0.511
	P_3	−0.98	−0.99	−1.42	−0.425
β-Cd_2P_3Cl	Cd	2.26	2.17	2.18	−0.087
	Cl	−2.00	−1.87	−1.07	0.924
	P_1	−0.88	−0.81	−1.42	−0.533
	P_2	−0.76	−0.85	−0.45	0.315
β-Cd_2P_3Br	Cd	2.40	2.31	2.18	−0.224
	Br	−2.09	−2.03	−1.05	1.035
	P_1	−0.90	−0.87	−1.43	−0.524
	P_2	−0.91	−0.84	−0.45	0.462
β-Cd_2P_3I	Cd	2.68	2.64	2.19	−0.489
	I	−2.32	−2.33	−1.07	1.242
	P_1	−0.99	−0.98	−1.42	−0.432
	P_2	−1.42	−0.99	−0.48	0.940

Table S8 Atomic bond-valence for α/β-Cd-P-X (X = Cl, Br, I) [2-3a].

Compound	Atom	X	Y	Z	BVS
α-Cd_2P_3Cl	Cd(1)	0.000	0.149	0.000	2.081
	Cd(2)	0.494	0.144	0.080	2.161
	P(1)	0.116	0.046	0.318	1.159
	P(2)	-0.258	0.296	0.038	1.342
	P(3)	0.366	0.045	-0.240	1.133
	Cl(1)	0.253	0.345	-0.004	0.690
α-Cd_2P_3Br	Cd(1)	0.000	0.147	0.000	2.217
	Cd(2)	0.504	0.147	0.080	2.122
	P(1)	0.130	0.038	0.315	1.080
	P(2)	-0.250	0.292	0.005	1.409
	P(3)	0.378	0.040	-0.210	1.198
	Br(1)	0.249	0.374	0.070	0.653
α-Cd_2P_3I	Cd(1)	0.000	0.141	0.000	1.892
	Cd(2)	0.500	0.145	0.069	2.386
	P(1)	0.147	0.043	0.324	0.897
	P(2)	-0.258	0.290	0.040	1.235
	P(3)	0.388	0.044	-0.239	1.175
	I(1)	0.240	0.374	0.060	0.971
β-Cd_2P_3Cl	Cd(1)	0.245	0.356	0.290	2.027
	P(1)	0.376	0.047	0.031	1.173
	P(2)	0.000	0.709	0.250	1.319
	Cl(1)	0.000	0.126	0.250	0.518
β-Cd_2P_3Br	Cd(1)	0.245	0.356	0.290	2.095
	P(1)	0.376	0.047	0.031	1.139
	P(2)	0.000	0.709	0.250	1.226
	Br(1)	0.000	0.126	0.250	0.684
β-Cd_2P_3I	Cd(1)	0.245	0.356	0.290	2.124
	P(1)	0.376	0.047	0.031	1.069
	P(2)	0.000	0.709	0.250	1.074
	I(1)	0.000	0.126	0.250	1.034

Table S9 Selected bond length for α/β-Cd-P-X (X = Cl, Br, I) [2-3a].

α-Cd_2P_3Cl		α-Cd_2P_3Br		α-Cd_2P_3I	
Cd(1)-P(1)	= 2.508	Cd(1)-P(1)	= 2.529	Cd(1)-P(1)	= 2.591
Cd(1)-P(1)	= 2.579	Cd(1)-P(1)	= 2.612	Cd(1)-P(1)	= 2.689
Cd(1)-P(2)	= 2.505	Cd(1)-P(2)	= 2.417	Cd(1)-P(2)	= 2.601
Cd(1)-Cl(1)	= 2.681	Cd(1)-Br(1)	= 2.863	Cd(1)-I(1)	= 2.923
Cd(1)-Cl(1)	= 3.363	Cd(1)-Br(1)	= 3.305	Cd(1)-I(1)	= 3.367
Cd(2)-P(3)	= 2.508	Cd(2)-P(3)	= 2.441	Cd(2)-P(3)	= 2.451
Cd(2)-P(3)	= 2.598	Cd(2)-P(3)	= 2.646	Cd(2)-P(3)	= 2.524
Cd(2)-P(2)	= 2.471	Cd(2)-P(2)	= 2.531	Cd(2)-P(2)	= 2.550
Cd(2)-Cl(1)	= 2.626	Cd(2)-Br(1)	= 2.907	Cd(2)-I(1)	= 3.019
Cd(2)-Cl(1)	= 3.423	Cd(2)-Br(1)	= 3.183	Cd(2)-I(1)	= 3.219
P(1)-P(2)	= 2.271	P(1)-P(2)	= 2.209	P(1)-P(2)	= 2.290
P(1)-P(3)	= 2.271	P(1)-P(3)	= 2.686	P(1)-P(3)	= 2.269
P(3)-P(2)	= 2.282	P(3)-P(2)	= 2.686	P(3)-P(2)	= 2.435
β-Cd_2P_3Cl		β-Cd_2P_3Br		β-Cd_2P_3I	
Cd(1)-P(1)	= 2.495	Cd(1)-P(1)	= 2.508	Cd(1)-P(1)	= 2.537
Cd(1)-P(1)	= 2.585	Cd(1)-P(1)	= 2.593	Cd(1)-P(1)	= 2.610
Cd(1)-P(2)	= 2.494	Cd(1)-P(2)	= 2.521	Cd(1)-P(2)	= 2.570
Cd(1)-Cl(1)	= 2.819	Cd(1)-Br(1)	= 2.854	Cd(1)-I(1)	= 2.920
Cd(1)-Cl(1)	= 3.224	Cd(1)-Br(1)	= 3.259	Cd(1)-I(1)	= 3.328
P(1)-P(1)	= 2.286	P(1)-P(1)	= 2.308	P(1)-P(1)	= 2.348
P(1)-P(2)	= 2.283	P(1)-P(2)	= 2.301	P(1)-P(2)	= 2.335

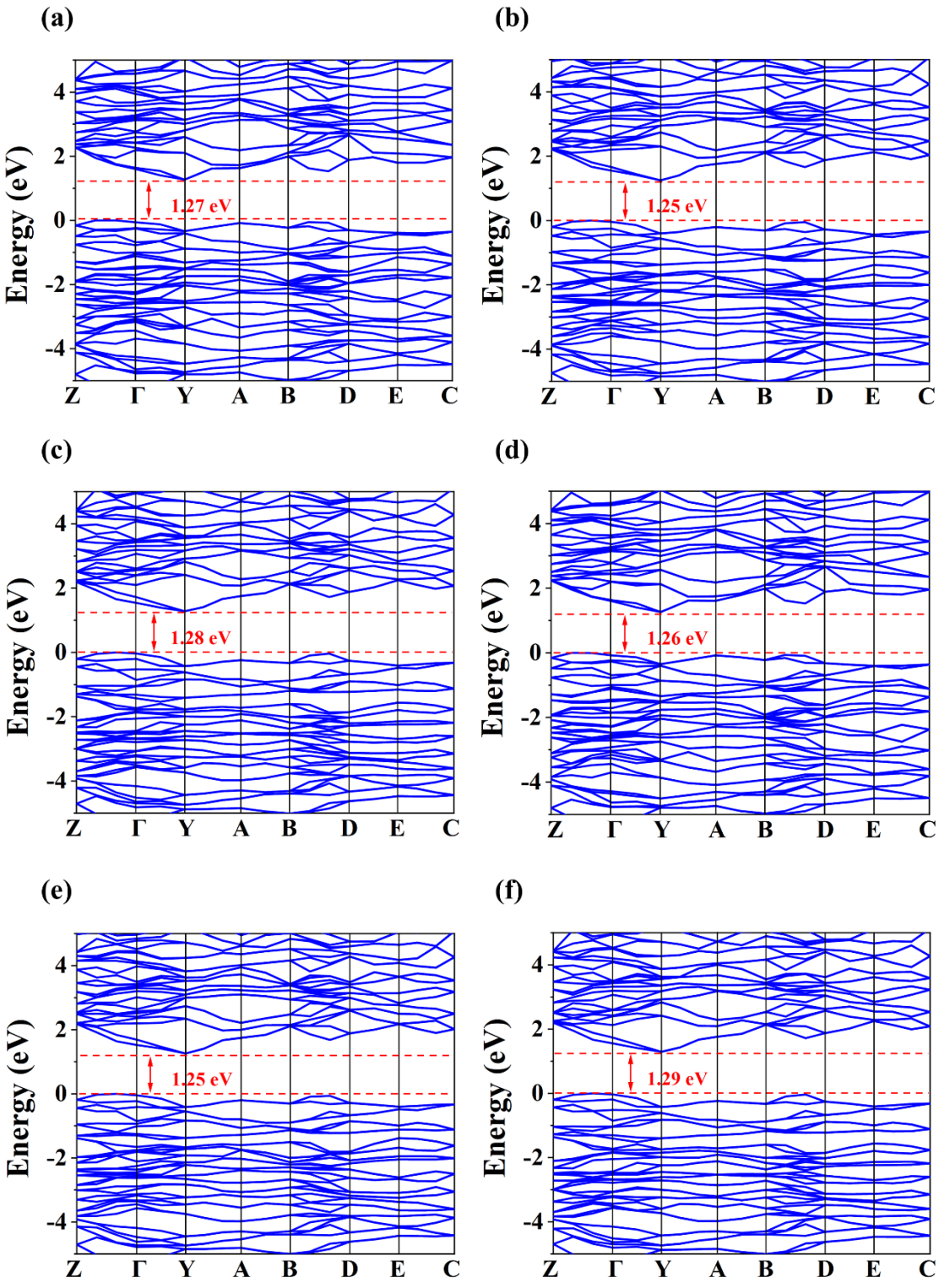
(a)
(b)
(c)
(d)
(e)
(f)
Energy (eV)
4
2
0
-2
-4
1.27 eV
1.25 eV
1.28 eV
1.26 eV
1.25 eV
1.29 eV
Z
Γ
Y
A
B
D
E
C

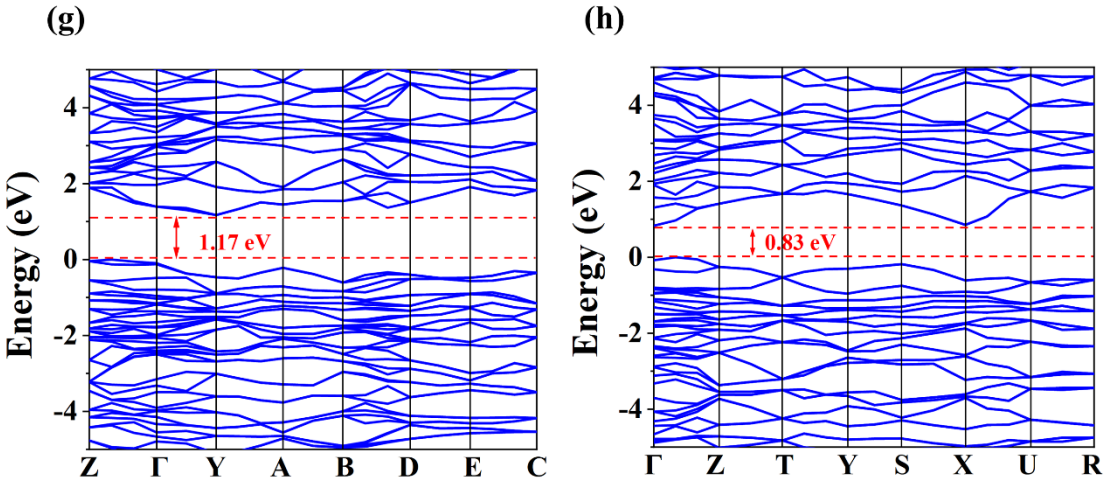

Figure S1 Calculated band gaps of α-Cd_2P_3Cl (a), α-Cd_2P_3Br (b), α-Cd_2P_3I (c), β-Cd_2P_3Cl (d), β-Cd_2P_3Br (e), β-Cd_2P_3I (f), Hg_2P_3Cl (g), and Hg_2P_3Br (h).

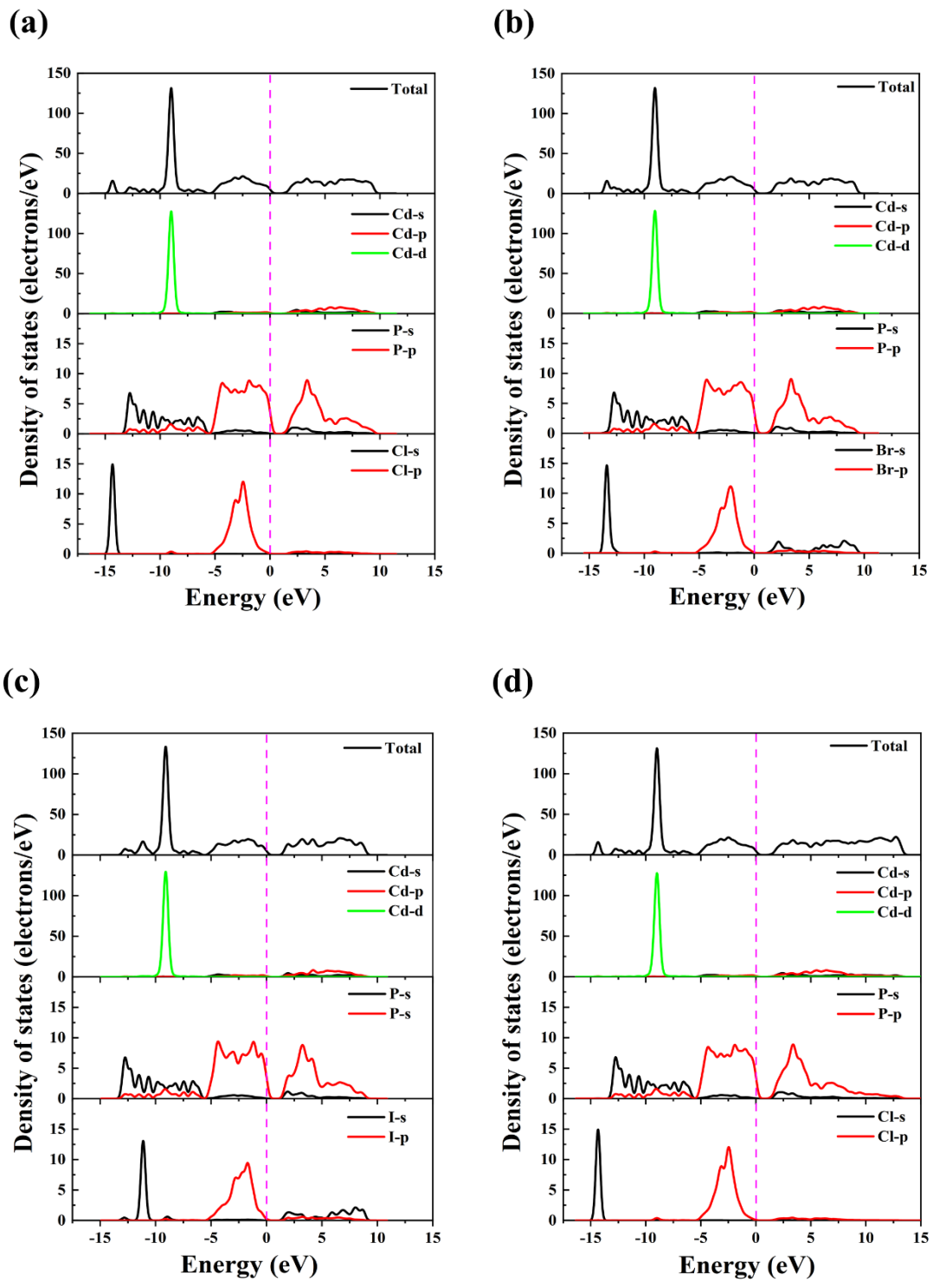
(a)
(b)
(c)
(d)
Total
Cd-s
Cd-p
Cd-d
P-s
P-p
Cl-s
Cl-p
Br-s
Br-p
I-s
I-p
Density of states (electrons/eV)
Energy (eV)

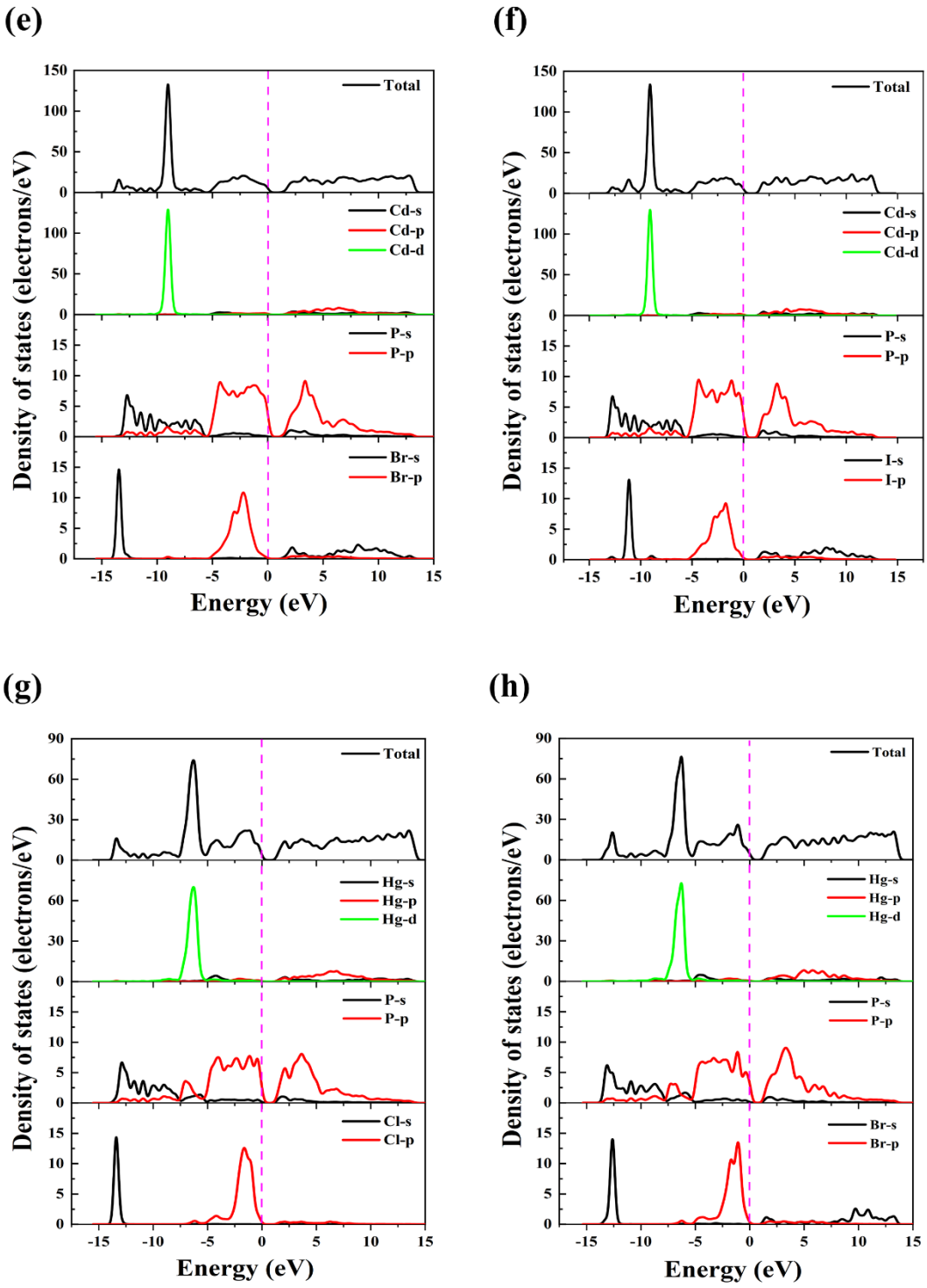

Figure S2 Total and partial density of states (T/PDOS) of α-Cd_2P_3Cl (a), α-Cd_2P_3Br (b), α-Cd_2P_3I (c), β-Cd_2P_3Cl (d), β-Cd_2P_3Br (e), β-Cd_2P_3I (f), Hg_2P_3Cl (g), and Hg_2P_3Br (h).

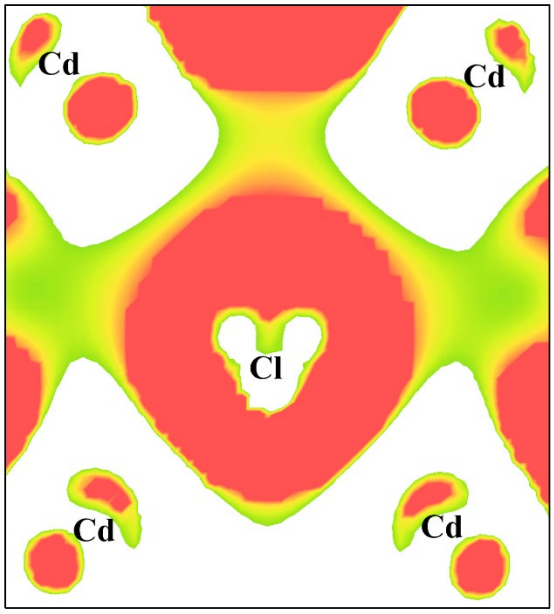

Figure S3 Electron-density difference maps for α-Cd_2P_3Cl.

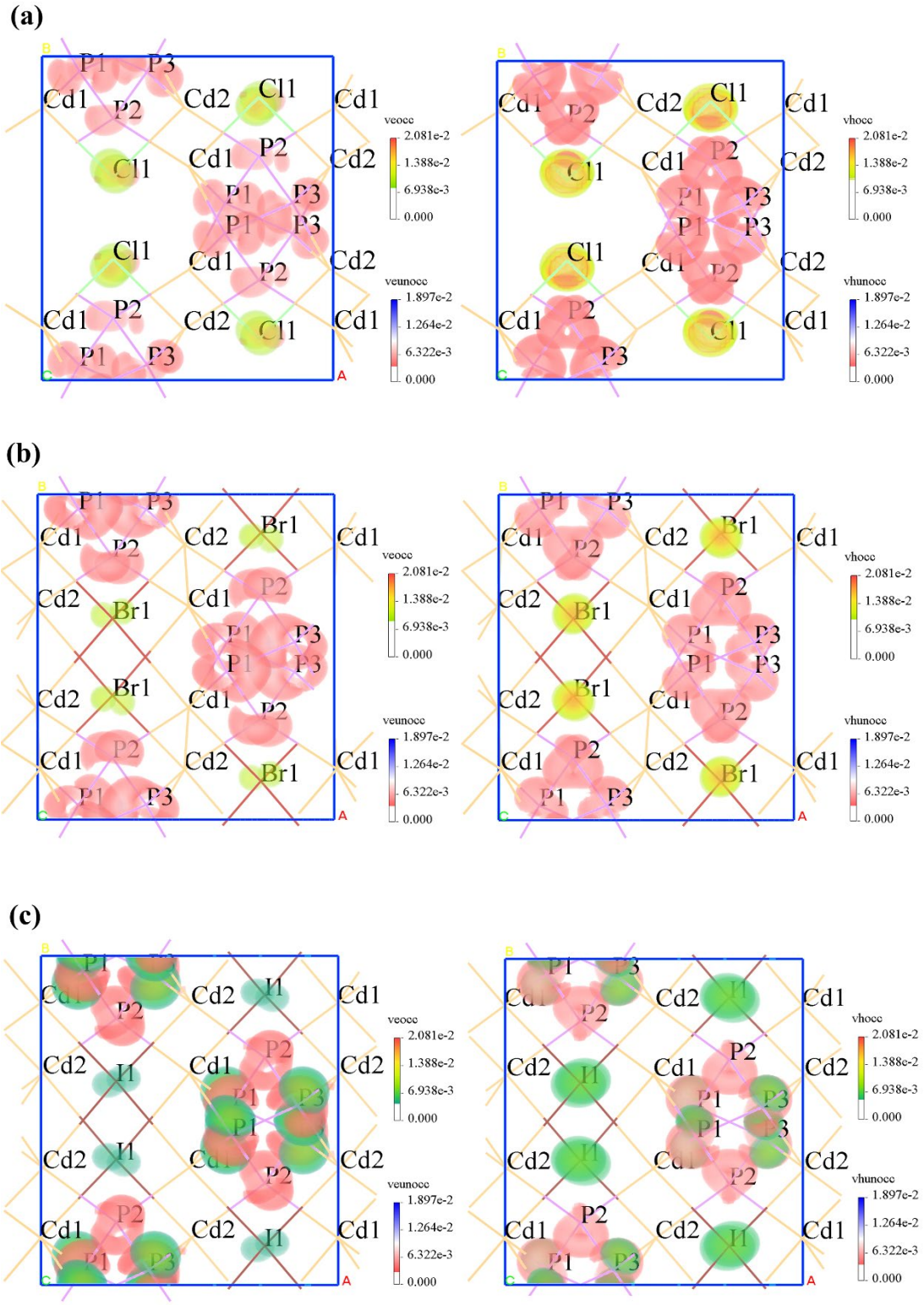

Figure S4 SHG-density of α-Cd_2P_3Cl (a), α-Cd_2P_3Br (b), and α-Cd_2P_3I (c).

Reference

[1] G. Walters, E. H. Sargent, Electrooptic Response in Germanium Halide Perovskites, *J. Phys. Chem. Lett*., 2018, **9**, 1018-1027.

[2] A. Rebbah, J. Yazbeck, R. Lande, A. Deschanvres, Etudes structurales et optiques des phases du type Cd_2A_3X (A= As, P; X= Cl, Br, I) et de leur solution solide, *Mater. Res. Bull*., 1981, **16**, 525-533.

[3] (a) P. C. Donohue, The Synthesis and Properties of Cd_2P_3Cl, Cd_2P_3Br, and Cd_2P_3I, *J. Solid State Chem*., 1972, **5**, 71-74; (b) A. Roy, A. Singh, S. A. Aravindh, S. Servottam, U. V. Waghmare, C. N. R. Rao, Structural Features and HER activity of Cadmium Phosphohalides, *Angew. Chem. Int. Ed.*, 2019, **58**, 6926-6931.

[4] A. V. Shevelkov, E. V. Dikarev, B. A. Popovkin, Helical $^1{}_\infty$Chains in the Structures of Hg_2P_3Br and Hg_2P_3Cl, *Z. Kristallogr.*, 1994, **209**, 583-585.

[5] T. Liu, J. G. Qin, G. Zhang, T. Zhu, F. Niu, Y. Wu, C. Chen, Mercury Bromide ($HgBr_2$): A Promising Nonlinear Optical Material in IR Region with a High Laser Damage Threshold, *Appl. Phys. Lett*., 2008, **93**, 091102-091106.

[6] X. Shi, Z. Ma, C. He, K. Wu, Strong SHG Responses Predicted in Binary Metal Halide Crystal HgI_2, *Chem. Phys. Lett*., 2014, **608**, 219-223.

[7] C. Barta, C. Barta Jr, Physical Properties of Single Crystals of the Calomel Gorup (Hg_2X_2: X = Cl, Br)[1], *Mater. Sci. Forum*., 1991, **61**, 93-150.

[8] M. Kars, T. Roisnel, V. Dorcet, A. Rebbah, O. D. Carlos, (2012). Redetermination of Hg_2I_2, *Acta Crystallogr. E*, 2012, **68**, i11-i11.

[9] K. Yamada, K. Isobe, T. Okuda, Y. Furukawa, Successive Phase Transitions and High Ionic Conductivity of Trichlorogermanate (II) Salts as Studied by 35C1 NQR and Powder X-Ray Diffraction. *Z. Naturforsch., A: Phys. Sci.*, 1994, **49**, 258-266.

[10] L. C. Tang, J. Y. Huang, C. S. Chang, M. H. Lee, L. Q. Liu, New Infrared Nonlinear Optical Crystal $CsGeBr_3$: Synthesis, Structure and Powder Second-Harmonic Generation Properties, *J. Phys.: Condens. Matter*., 2005, **17**, 7275-7286.

[11] C. C. Stoumpos, L. Frazer, D. J. Clark, Y. S. Kim, S. H. Rhim, A. J. Freeman, J. B. Ketterson, J. I. Jang, M. G. Kanatzidis, Hybrid Germanium Iodide Perovskite Semiconductors: Active Lone Pairs, Structural Distortions, Direct and Indirect Energy Gaps, and Strong Nonlinear Optical Properties, *J. Am. Chem. Soc*., 2015, **137**, 6804-6819.

[12] M. R. Linaburg, E. T. McClure, J. D. Majher, P. M. Woodward, $Cs_{1-x}Rb_xPbCl_3$ and $Cs_{1-x}Rb_xPbBr_3$ Solid Solutions: Understanding Octahedral Tilting in Lead Halide Perovskites, *Chem. Mater*., 2017, **29**, 3507-3514.

[13] R. J. Sutton, M. R. Filip, A. A. Haghighirad, N. Sakai, B. Wenger, F. Giustino, H. J. Snaith, Cubic or Orthorhombic? Revealing the Crystal Structure of Metastable Black-Phase $CsPbI_3$ by Theory and Experiment, *ACS Energy Lett*., 2018, **3**, 1787-1794.

[14] P. Schwarz, J. Wachter, M. Zabel, PAs_3S_3 cage as a new building block in copper halide coordination polymers, *Inorg. Chem*., 2011, **50**, 8477-8483.

[15] G. Zhang, J. G. Qin, T. Liu, Y. J. Li, Y. C. Wu, C. T. Chen, $NaSb_3F_{10}$: A New Second-Order Nonlinear Optical Crystal to be Used in the IR Region with Very High Laser Damage Threshold, *Appl. Phys. Lett*., 2009, **95**, 261104-261104.

[16] L. Kang, D. M. Ramo, Z. S. Lin, P. D. Bristowe, J. G. Qin, C. T. Chen, First Principles Selection and Design of Mid-IR Nonlinear Optical Halide Crystals, *J. Mater. Chem. C*, 2013, **1**, 7363-7370.

[17] G. Zhang, T. Liu, T. X. Zhu, J. G. Qin, Y. C. Wu, C. T. Chen, SbF_3: A New Second-Order Nonlinear Optical Material, *Opt. Mater*., 2008, **31**, 110-113.

[18] J. Y. Guo, A. Tudi, S. J. Han, Z. H. Yang, S. L. Pan, $Sn_2B_5O_9Cl$: A Material with Large Birefringence Enhancement Activated Prepared via Alkaline-Earth-Metal Substitution by Tin, *Angew. Chem. Int. Ed.*, 2019, **58**, 17675-17678.

[19] J. Y. Guo, S. C. Cheng, S. J. Han, Z. H. Yang, S. L. Pan, $Sn_2B_5O_9Br$ as an Outstanding Bifunctional Material with Strong Second-Harmonic Generation Effect and Large Birefringence, *Adv. Opt. Mater*., 2021, **9**, 2001734-2001740.

[20] B.V.Egorova, A. V. Olenev, P. S. Berdonosov, A. N. Kuznetsov, S. Yu. Stefanovich, V. A. Dolgikh, T. Mahenthirarajah, P. Lightfoot, Lead-strontium Borate Halides with Hilgardite-type Structure and their SHG Properties, *J. Solid State Chem.*, 2008, **181,** 1891-1898.

[21] E. L. Belokoneva, A. G. Al-Ama, S. Y. Stefanovich, P. A. Plachinda, Crystal Structure of the Lead Bromo-Borate $Pb_2[B_5O_9]Br$ from Precision Single-Crystal X-ray Diffraction Data and the Problem of Optical Nonlinearity of Hilgardites, *Crystallogr. Rep*., 2007, **52**, 795-800.

[22] Y. Z. Huang, L. M. Wu, X. T. Wu, L. H. Li, L. Chen, Y. F. Zhang, $Pb_2B_5O_9I$: An Iodide Borate with Strong Second Harmonic Generation, *J. Am. Chem. Soc*., 2010, **132**, 12788-12789.

[23] L. Liu, B. B. Zhang, F. F. Zhang, S. L. Pan, F. Y. Zhang, X. W. Zhang, X. Y. Dong, Z. H. Yang, $Pb_6Ba_2(BO_3)_5X$ (X= Cl, Br): New Borate Halides with Strong Predicted Optical Anisotropies Derived from Pb^{2+} and $(BO_3)^{3-}$, *Dalton Trans*., 2015, **44**, 7041-7047.